A Lagrangian Dual Approach for Identifying the Worst Contingencies in Power Systems

Brian Dandurand* Kibaek Kim† Sven Leyffer‡

July 25, 2019

Abstract

We address the problem of identifying critical contingencies in an electric grid network. The critical contingency identification is modeled as a nonconvex robust optimization problem, where the upper level must choose the most damaging attack that anticipates the lower-level decision to minimize the damage from the attacks. In general, nonconvex robust optimization problems are NP-hard, and effective solution approaches make use of the problem structure. Initially, we consider a single-level reformulation to the original problem, but we note that its convexity properties do not allow for tractable solution approaches. To address this issue, we pose a Lagrangian-based reformulation that preserves the modeling of nonlinear aspects of the power network operation, while having the desired structure amenable to the application of standard solution approaches in mixed-integer convex programming. We present computational experiments based on IEEE and Pegase cases, discuss the effectiveness of the new approach, and conclude with questions arising from the experiments that can be addressed in the future.

Keywords. Optimal power flow, nonconvex robust optimization, network contingency identification, mixed-integer convex programming

AMS subject classifications. 90C06, 90C11, 90C22, 90C30, 90C47, 90C56, 90C57, 90C90

1 Introduction

We present solution methods for application to the problem of identifying the critical contingencies in an alternating current power system. We model the problem as a Stackelberg game, where the attacker (i.e., leader) aims to compromise the functionality of a small subset of components whose failure or malfunction results in a system disruption that cannot be adequately remedied with available defensive measures by a defender (i.e., follower). An attack need not come from a malevolent adversary but may come from a "perfect storm" of naturally occurring component failures. One example of where a small number of component failures had significant consequence was during the large-scale blackout in the northeastern United States and neighboring parts of Canada in the summer of 2003 [U.S04, NER04].

We consider a power system network with sets of buses and lines, whose index sets are denoted by N and L, respectively. We focus on the contingencies associated with the cutting of network lines. For each line $l \in L$, let x_l be the binary decision variable indicating whether the line l is cut ($x_l = 1$) or not ($x_l = 0$). We model the bilevel contingency identification problem as follows:

$$\Phi := \max_{x} \left\{ \phi(x) \quad \text{s.t.} \quad \sum_{l \in L} x_l \leq K, \quad x_l \in \{0,1\},\ l \in L \right\}, \tag{1}$$

where $x \mapsto \phi(x)$ for a given $x := (x_l)_{l \in L} \in \{0,1\}^{|L|}$ is a nonnegative-valued function whose value is determined by solving a lower-level optimization for the minimal value of system infeasibility due to a defender's optimal response to attack x. In the upper-level problem (1), the attacker is restricted by the budget $\sum_{l \in L} x_l \leq K$ for nonnegative integer K. Problem (1) is given as the *optimal value transformation* of a bilevel optimization problem (see [DKPVK15], Sections 1.4 and 3.6, and references therein). When the underlying network

*Argonne National Laboratory, bdandurand@anl.gov
†Argonne National Laboratory, kimk@anl.gov
‡Argonne National Laboratory, leyffer@mcs.anl.gov

model includes the AC power flow equations, we set $\phi = \phi^{AC}$, and the optimal value to (1) with $\phi = \phi^{AC}$ is denoted by Φ^{AC}. Aside from its bilevel nature, problem (1) with $\phi = \phi^{AC}$ is challenging because the AC electric system of the lower-level problem is nonlinear and nonconvex. Correspondingly, $x \mapsto \phi^{AC}(x)$ and its associated defender subproblem have no identifiable convexity structure. Without such structure, any solution approach to (1) cannot skip the combinatorial enumeration of the feasible solution set.

Consequently, we consider convex relaxations of the AC power balance constraints. For the semidefinite programming (SDP) relaxation [BWFW08, LL12] of the defender subproblem, we set $\phi = \phi^{SDP}$. Analogously, for the second-order cone (SOC) relaxation [Jab06], we set $\phi = \phi^{SOC}$. The corresponding optimal values to (1) with $\phi = \phi^{SDP}$ and $\phi = \phi^{SOC}$ are denoted by Φ^{SDP} and Φ^{SOC}, respectively.

Earlier efforts involved developing methods applied to linearizations and/or direct current approximations of the underlying AC network (e.g., [SWB09, Arr10, ZZ13, Kim17, BV10]). We avoid these approaches, because they oversimplify the AC power flow balance equations, resulting in inaccurate assessments of network vulnerabilities.

Other approaches that address nonlinear models of the AC network rely on other simplifying assumptions. These assumptions allow for solution approaches based on solving the Karush-Kuhn-Tucker (KKT) reformulation and/or allow for the approximation of the problem in mixed-integer linear programming [PMDL10]. However, such KKT-reformulated problems are well known to violate constraint qualification at every feasible point. Mixed-integer linear reformulations of the complementarity constraints within the KKT system may be employed to overcome this issue. However, the continuous relaxation to such reformulations does not provide good bounds for the effective use of a branch-and-bound approach.

Most recently, Wu et al. [WCA18] posed a dual-solution approach based on SOC relaxation [Jab06]. SOC relaxations of the AC power flow balance equations are substantially more accurate than DC or other linear relaxations or approximations, but they are not as accurate as SDP relaxations. Solution approaches applied to SOCs tend to scale better than those applied to SDPs but do not scale as well as linear solution approaches. Our research goal, therefore, is to improve the accuracy of the SOC relaxation approach of [WCA18] by employing other relaxations that are nevertheless amenable to linear solution approaches for improving scalability.

In this paper we present a new solution approach to solving problem (1). The key contributions of this paper are summarized as follows:

1. We present a new single-level reformulation of (1) based on the Lagrangian dual of ϕ^{AC} using techniques simimlar to those described in [Pha12].

2. We prove that the Lagrangian relaxation of ϕ^{AC} provides a dual bound of ϕ^{AC} that is as tight as that of ϕ^{SDP} and hence tighter than that of ϕ^{SOC}.

3. We develop a method by applying a single-tree variant of the extended cutting plane (ECP) algorithm [WP95a, EMW14] to our single-level reformulation with the proof of its finite, globally optimal convergence.

4. We develop a new structured relaxation of the optimal power flow defender subproblem that allows for the development of a new method that scales to larger test instances than previous methods do.

The single-level reformulation for the first contribution is a mixed-binary concave maximization problem having only one nonlinear nonsmooth constraint. As needed for implementing the third contribution, values and subgradients associated with the corresponding constraint function are obtained by solving a quadratic trust-region subproblem that, although nonconvex, can be solved to global optimality using well-known approaches; see, for example, [Hag01]. The new structure-based relaxation of the fourth contribution relaxes the equations governing the AC power flows between two buses connected by an active line given bus voltages, while maintaining power flow balance as required by Kirchoff's Law. We propagate this relaxation into the single-level reformulation described above, resulting in a modified single-level reformulation. Computational results show that the new method resulting from the application of the single-tree ECP algorithm to the modified single-level reformulation scales to larger instances than does the SOC relaxation approach in [WCA18], while maintaining the accuracy of the SOC relaxation approach for most test instances.

For baseline comparison purposes, we also implement the single-level reformulations based on the SDP and SOC relaxations of the lower-level subproblem (i.e., ϕ^{SDP} and ϕ^{SOC}, respectively). For the SDP approach, we implement a simple branch-and-bound approach applied to the SDP-based reformulation. The branching rule is informed by the guidelines in [GPU18, Section 8.2]. We steer away from using only maximum fractionality

for the branching rule, because of the typically big search tree that is generated. For our application of interest, the solution of each SDP node subproblem is expensive, so strong branching is not practical. Hence, our own branching rule tries to emulate pseudocost branching using the physical information present in the line flow admittance parameters. For the SOC approach, we apply a conic solver to the SOC-based reformulation as done in [WCA18].

This paper is organized as follows. In Section 2, we present the bilevel model formulation with the lower-level problem $\phi(x)$ of AC optimal power flow and develop the single-level reformulation based on the Lagrangian dual of $\phi(x)$. In Section 3, we analyze the strength of our Lagrangian dual subproblem by comparing it with the SDP and SOC relaxations of the underlying AC power system. Additionally, we describe the structured relaxation of the fourth contribution and the modified single-level reformulation that is obtained from it. In section 4, we describe the single-tree generalized ECP algorithm, analyze its convergence properties, and justify its application to the Lagrangian dual-based reformulation of problem (1). We additionally describe the methods resulting from the application of conic optimization solvers to the SDP- and SOC-based reformulations, where we provide a simple branch-and-bound framework to the former. Section 5 reports the numerical results from the different methods on different power grid instances. We present and comment on numerical results from the different approaches with respect to the various profiles related to solution times, solution qualities, number of branch-and-cut nodes, and number of applied cutting planes. In Section 6, we summarize our conclusions and describe future work

2 Single-Level Reformulation

In this section, we present single-level reformulations of problem (1) based on Lagrangian relaxations of the lower-level problem with respect to some of the constraints. To begin, we specify the lower-level AC optimal power flow (ACOPF) with details of the power flow physics. We follow the development of Chapter 3 in [ZMS18].

2.1 Nonconvex Lower-Level ACOPF Problem

For each line $(i,j) = l \in L$ connected from bus i to bus j, we define the complex-valued line admittance z_l^{-1}, which is the inverse of the line impedance $z_l := (r_l + \mathfrak{i}\chi_l)$ for a given resistance r_l and reactance χ_l. The imaginary component of any complex number is denoted $\mathfrak{i} := \sqrt{-1}$. We denote complex current flows by ι_l^f and ι_l^t, where the superscripts f and t indicate the forward and backward direction of flows, respectively. Given complex bus voltages v_i, $i \in N$, the current flows are determined by

$$\begin{bmatrix} \iota_l^f \\ \iota_l^t \end{bmatrix} := \begin{bmatrix} Y_l^{ff} & Y_l^{ft} \\ Y_l^{tf} & Y_l^{tt} \end{bmatrix} \begin{bmatrix} v_i \\ v_j \end{bmatrix}, \tag{2}$$

where

$$Y_l := \begin{bmatrix} Y_l^{ff} & Y_l^{ft} \\ Y_l^{tf} & Y_l^{tt} \end{bmatrix} := \begin{bmatrix} (z^{-1} + \mathfrak{i}\frac{b_l}{2})\frac{1}{\tau_l^2} & -z_l^{-1}\frac{1}{\tau_l e^{-\mathfrak{i}\psi_l}} \\ -z_l^{-1}\frac{1}{\tau_l e^{\mathfrak{i}\psi_l}} & z_l^{-1} + \mathfrak{i}\frac{b_l}{2} \end{bmatrix} \tag{3}$$

after defining, for each line $l \in L$, the charging susceptance b_l, the tap ratio τ_l, and the phase angle shift ψ_l. At each line $(i,j) = l \in L$, complex power flows from bus i and to bus j are respectively given by

$$s_l^f := v_i(\iota_l^f)^* = v_i v_i^*(Y_l^{ff})^* + v_i v_j^*(Y_l^{ft})^*, \;\; s_l^t := v_j(\iota_l^t)^* = v_j v_i^*(Y_l^{tf})^* + v_j v_j^*(Y_l^{tt})^*, \tag{4}$$

where the $*$ operator applied to the vector corresponds to componentwise conjugacy in complex arithmetic and v_i is a complex voltage at bus i. We introduce $W \in \mathbb{C}^{|N|\times|N|}$, where each element $W_{ij} = v_i v_j^*$, $i,j \in N$. By defining $v := [v_i]_{i\in N} \in \mathbb{C}^{|N|}$, we may also write $W = vv^*$, which is a rank 1 matrix. For each line $(i,j) = l \in L$, we define the following 2×2 submatrices of W:

$$W_l := \begin{bmatrix} W_{ii} & W_{ij} \\ W_{ji} & W_{jj} \end{bmatrix}. \tag{5}$$

In light of these definitions, we write each line $(i,j) = l \in L$ complex power flow as linear functions of W_l given by

$$s_l^f(W_l) = W_{ii}(Y_l^{ff})^* + W_{ij}(Y_l^{ft})^*, \qquad s_l^t(W_l) = W_{ji}(Y_l^{tf})^* + W_{jj}(Y_l^{tt})^*. \tag{6}$$

Denoting $v_i^R := \Re\{v_i\}$ and $v_i^I := \Im\{v_i\}$, $i \in N$, we define

$$W_{ij}^R := \Re\{W_{ij}\} = v_i^R v_j^R + v_i^I v_j^I, \quad W_{ij}^I := \Im\{W_{ij}\} = v_j^R v_i^I - v_i^R v_j^I, \quad i,j \in N. \tag{7}$$

Note that $W_{ii}^R = (e_i^R)^2 + (e_i^I)^2 = |V_i|^2$ and $W_{ii}^I = 0$, so that $W_{ii} = W_{ii}^R$ for each bus $i \in N$. Also, we define for each line $l \in L$

$$p_l^f(W_l) := \Re\{s_l^f(W_l)\}, \quad p_l^t(W_l) := \Re\{s_l^t(W_l)\} \tag{8a}$$

$$q_l^f(W_l) := \Im\{s_l^f(W_l)\}, \quad q_l^t(W_l) := \Im\{s_l^t(W_l)\}. \tag{8b}$$

For each bus $i \in N$, the shunt power injection is given by the linear function of W_{ii},

$$p_i^{sh}(W_{ii}) := Y_i^{shR} W_{ii}, \qquad q_i^{sh}(W_{ii}) := -Y_i^{shI} W_{ii}, \tag{8c}$$

where Y_i^{shR} and Y_i^{shI} are, respectively, the real and imaginary components of the shunt admittance at bus $i \in N$.

We present the defender's lower-level problem that seeks to enforce power flow balance. Let p_i^N and q_i^N be the net active and reactive power injections, respectively, to each bus $i \in N$, given by

$$p_i^N(W,x) := p_i^{sh}(W_{ii}) + \sum_{l \in L_i^f} (1 - x_l)\, p_l^f(W_l) + \sum_{l \in L_i^t} (1 - x_l)\, p_l^t(W_l), \tag{9a}$$

$$q_i^N(W,x) := q_i^{sh}(W_{ii}) + \sum_{l \in L_i^f} (1 - x_l)\, q_l^f(W_l) + \sum_{l \in L_i^t} (1 - x_l)\, q_l^t(W_l), \tag{9b}$$

where L_i^f is the set of lines with the origin of bus i and L_i^t is the set of lines with the destination of bus i. Active power generation and reactive power generation at bus $i \in N$ are denoted by p_i^G and q_i^G, respectively, while active and reactive power demands at bus $i \in N$ is denoted by P_i^D and Q_i^D. Power generation is constrained to the bounds

$$P_i^{min} \le p_i^G \le P_i^{max}, \quad Q_i^{min} \le q_i^G \le Q_i^{max}, \quad i \in N. \tag{10}$$

With these definitions, the power flow balance equations are given by

$$p_i^N(W,x) = p_i^G - P_i^D \tag{11a}$$

$$q_i^N(W,x) = q_i^G - Q_i^D. \tag{11b}$$

The defender attempts to enforce the power flow balance equations (11) by adjusting power flow control W and power generations $p^G := (p_i^G)_{i \in N}$, $q^G := (q_i^G)_{i \in N}$ for a given line contingency x. Note, however, that for a given attack x, it may not be possible to enforce constraints (11) by feasible adjustments of W, p^G, and q^G. That is, load shedding or excessive power generation might be unavoidable. Consequently, we model the lower-level defender subproblem to minimize the use of load shedding and/or excessive power generation to enforce the power flow balance equations (11). The lower-level defender's subproblem is modeled by

$$\phi^{AC}(x) := \min_{v,W,p^G,q^G,u} \quad \sum_{i \in N} (u_i^p + u_i^q + u_i^m) \tag{12a}$$

$$\text{s.t.} \quad W = vv^* \tag{12b}$$

$$u := (u_i^p, u_i^q, u_i^m)_{i \in N} \ge 0 \tag{12c}$$

$$P_i^{min} \le p_i^G \le P_i^{max}, \quad Q_i^{min} \le q_i^G \le Q_i^{max}, \quad i \in N \tag{12d}$$

$$-u_i^p \le p_i^N(W,x) - p_i^G + P_i^D \le u_i^p, \quad i \in N, \tag{12e}$$

$$-u_i^q \le q_i^N(W,x) - q_i^G + Q_i^D \le u_i^q, \quad i \in N, \tag{12f}$$

$$(V_i^{min})^2 - u_i^m \le W_{ii} \le (V_i^{max})^2 + u_i^m, \quad i \in N, \tag{12g}$$

where v, W, p^G, q^G, u are decision variables. In (12), power flow balance constraints (12e)–(12f) and the voltage bound constraint (12g) are treated as soft constraints with auxiliary variables $u_i := (u_i^p, u_i^q, u_i^m)$ that are penalized in the objective function. The auxiliary variables u_i^p and u_i^q can be interpreted as either demand load shedding or excess power generation at each bus $i \in N$. For constraint (12g), recall that $W_{ii} = |v_i|^2$. Hence, the lower-level problem minimizes the constraint violations of (12e)–(12g). Note that for $x = 0$, $\phi^{AC}(x)$ solves the ACOPF feasibility problem under ordinary (i.e., noncontingent) operating conditions. The resulting lower-level problem is a nonconvex nonlinear program due to the quadratic rank 1 constraint $W = vv^*$, while all the other constraints are linear.

2.2 Mixed-binary Lagrangian Relaxation

Problem (1) with the nonconvex lower-level problem (12) is nonsmooth and discrete. We develop a single-level reformulation based on the Lagrangian relaxation of the lower-level problem with respect to the soft constraints (12e)-(12g) (i.e., power flow constraints and voltage magnitude bounds) and the power generation bounds (12d). Introducing the corresponding nonnegative Lagrange multipliers $\alpha_i^+, \alpha_i^-, \beta_i^+, \beta_i^-, \gamma_i^+, \gamma_i^- \geq 0$, and $\delta_i^{p,+}, \delta_i^{p,-}, \delta_i^{q,+}, \delta_i^{q,-} \geq 0$ for $i \in N$, the Lagrangian dual problem is given by

$$\Phi_D^{AC} := \max_{x,\alpha,\beta,\gamma,\delta} \quad \phi_D^{AC}(x) \tag{13a}$$

$$\text{s.t.} \quad \sum_{l \in L} x_l \leq K, \quad x_l \in \{0,1\}, \quad l \in L \tag{13b}$$

$$\alpha_i^+, \alpha_i^-, \beta_i^+, \beta_i^-, \gamma_i^+, \gamma_i^- \geq 0, \quad i \in N \tag{13c}$$

$$\delta_i^{p,+}, \delta_i^{p,-}, \delta_i^{q,+}, \delta_i^{q,-} \geq 0, \quad i \in N, \tag{13d}$$

where $\phi_D^{AC}(x)$ represents the Lagrangian relaxation of $\phi^{AC}(x)$ with respect to constraints (12e)-(12g) and (12d) and is given by

$$\begin{aligned}
\phi_D^{AC}(x) = \min_{p^G, q^G, v, W, u} \; & \sum_{i \in N} \left[(\alpha_i^+ - \alpha_i^-)(p_i^N(W,x) - p_i^G + P_i^D) \right] \\
& + \sum_{i \in N} \left[(\beta_i^+ - \beta_i^-)(q_i^N(W,x) - q_i^G + Q_i^D) \right] \\
& + \sum_{i \in N} \left[(1 - \alpha_i^+ - \alpha_i^-) u_i^p + (1 - \beta_i^+ - \beta_i^-) u_i^q \right] \\
& + \sum_{i \in N} \left[\gamma_i^+ (W_{ii} - (V_i^{max})^2) + \gamma_i^- ((V_i^{min})^2 - W_{ii}) \right] \\
& + \sum_{i \in N} \left[(1 - \gamma_i^+ - \gamma_i^-) u_i^m \right] \\
& + \sum_{i \in N} \left[\delta_i^{p,+}(p_i^G - P_i^{max}) - \delta_i^{p,-}(p_i^G - P_i^{min}) \right] \\
& + \sum_{i \in N} \left[\delta_i^{q,+}(q_i^G - Q_i^{max}) - \delta_i^{q,-}(q_i^G - Q_i^{min}) \right] \\
\text{s.t. } & W = vv^*, \quad u^p, u^q, u^m \in \mathbb{R}_+^{|N|}.
\end{aligned} \tag{14}$$

Note that by weak duality, $\Phi^{AC} \geq \Phi_D^{AC}$.

The variables u, p^G, and q^G appear only in the objective function of (14), and the following conditions are necessary for the problem (14) to be bounded from below (i.e., the boundedness of the Lagrangian dual problem):

$$1 - \alpha_i^+ - \alpha_i^- \geq 0, \quad 1 - \beta_i^+ - \beta_i^- \geq 0, \quad 1 - \gamma_i^+ - \gamma_i^- \geq 0, \quad i \in N \tag{15a}$$

$$-\alpha_i^+ + \alpha_i^- + \delta_i^{p,+} - \delta_i^{p,-} = 0, \quad -\beta_i^+ + \beta_i^- + \delta_i^{q,+} - \delta_i^{q,-} = 0, \quad i \in N. \tag{15b}$$

With the conditions (15), the terms in u, p^G, and q^G can be dropped from the objective function of the inner minization problem. Moreover, by substituting

$$\alpha_i = \alpha_i^+ - \alpha_i^- \quad \text{and} \quad \beta_i = \beta_i^+ - \beta_i^-, \tag{16}$$

the Lagrangian dual problem (13) is equivalent to

$$\max_{x,\alpha,\beta,\gamma,\delta} \min_{v,W} \left\{ \begin{array}{c} \sum_{i\in N}\left[\alpha_i(p_i^N(W,x)+P_i^D)+\beta_i(q_i^N(W,x)+Q_i^D)\right] \\ +\sum_{i\in N}\left[(\gamma_i^+-\gamma_i^-)W_{ii}\right] \text{ s.t. } W=vv^* \end{array} \right\} \tag{17a}$$

$$+\sum_{i\in N}\left[-\delta_i^{p,+}P_i^{max}+\delta_i^{p,-}P_i^{min}-\delta_i^{q,+}Q_i^{max}+\delta_i^{q,-}Q_i^{min}\right]$$

$$+\sum_{i\in N}\left[\gamma_i^-(V_i^{min})^2-\gamma_i^+(V_i^{max})^2\right]$$

$$\text{s.t.} \sum_{l\in L} x_l \le K, \quad x_l\in\{0,1\}, \quad l\in L \tag{17b}$$

$$-1\le\alpha_i\le 1, \quad -1\le\beta_i\le 1, \quad \gamma_i^+ +\gamma_i^-\le 1, \quad \gamma_i^+,\gamma_i^-\ge 0 \quad i\in N, \tag{17c}$$

$$\delta_i^{p,+}-\delta_i^{p,-}=\alpha_i, \quad \delta_i^{q,+}-\delta_i^{q,-}=\beta_i, \quad \delta_i^{p,+},\delta_i^{p,-},\delta_i^{q,+},\delta_i^{q,-}\ge 0, \quad i\in N. \tag{17d}$$

The inner minimization problem in (17) is not convex because of the bilinear objective function and nonconvex quadratic constraints $W = vv^*$. Introducing auxiliary variables $\lambda_l^f, \lambda_l^t, \mu_l^f, \mu_l^t$, we linearize the bilinear terms by substituting

$$\lambda_l^f = (1-x_l)\alpha_i, \quad \lambda_l^t = (1-x_l)\alpha_j, \quad \mu_l^f = (1-x_l)\beta_i, \quad \mu_l^t = (1-x_l)\beta_j. \tag{18}$$

Using the McCormick [McC76] inequalities, we can rewrite the bilinear constraints (18) equivalently as the linear set of inequalities

$$\alpha_i - x_l \le \lambda_l^f \le \alpha_i + x_l, \qquad \alpha_j - x_l \le \lambda_l^t \le \alpha_j + x_l \tag{19a}$$

$$\beta_i - x_l \le \mu_l^f \le \beta_i + x_l, \qquad \beta_j - x_l \le \mu_l^t \le \beta_j + x_l \tag{19b}$$

$$-(1-x_l) \le \lambda_l^f \le (1-x_l), \qquad -(1-x_l) \le \lambda_l^t \le (1-x_l) \tag{19c}$$

$$-(1-x_l) \le \mu_l^f \le (1-x_l), \qquad -(1-x_l) \le \mu_l^t \le (1-x_l). \tag{19d}$$

Note that under the assumption $x_l \in \{0,1\}$, $l \in L$, the inequalities (19) equivalently represent the bilinear terms (18) and are not mere relaxations of (18). We define a polytope

$$\Pi := \left\{(x,\pi)\in[0,1]^{|L|}\times\mathbb{R}^{8|N|}\times\mathbb{R}^{4|L|} : (17c)-(17d),(19)\right\}, \tag{20}$$

where $\pi := (\alpha,\beta,\gamma,\delta,\lambda,\mu)$. Substituting $W = vv^*$ and collecting the vv^* terms, we rewrite the dual problem (17) as

$$\Phi_D^{AC} = \max_{x,\pi} \sum_{i\in N}\left[\alpha_i P_i^D+\beta_i Q_i^D-\gamma_i^+(V_i^{max})^2+\gamma_i^-(V_i^{min})^2\right] \tag{21}$$

$$+\sum_{i\in N}\left[-\delta_i^{p,+}P_i^{max}+\delta_i^{p,-}P_i^{min}-\delta_i^{q,+}Q_i^{max}+\delta_i^{q,-}Q_i^{min}\right]$$

$$+\min_{v\in\mathbb{C}^{|N|}} v^*H(\pi)v$$

$$\text{s.t.} \sum_{l\in L} x_l \le K, \quad x_l\in\{0,1\}, \quad l\in L, \quad (x,\pi)\in\Pi$$

where the Hermitian matrix $H(\pi)$, parameterized by π, is given by

$$H_{ii}(\pi) = \gamma_i^+ - \gamma_i^- + \alpha_i Y_i^{shR} - \beta_i Y_i^{shI} \tag{22a}$$

$$+\sum_{l\in L_i^f}\left(\lambda_l^f Y_l^{ffR}-\mu_l^f Y_l^{ffI}\right)+\sum_{l\in L_i^t}\left(\lambda_l^t Y_l^{ttR}-\mu_l^t Y_l^{ttI}\right) \quad i\in N$$

$$H_{ij}(\pi) = 0.5\left(\lambda_l^f Y_l^{ftR}-\mu_l^f Y_l^{ftI}+\lambda_l^t Y_l^{tfR}-\mu_l^t Y_l^{tf}\right) \tag{22b}$$

$$-0.5\mathfrak{i}\left(\lambda_l^f Y_l^{ftI}+\mu_l^f Y_l^{ftR}-\lambda_l^t Y_l^{tfI}-\mu_l^t Y_l^{tfR}\right) \quad (i,j)=l\in L$$

$$H_{ij}(\pi) = H_{ji}^*(\pi) \quad i,j\in N, \qquad H_{ij}(\pi)=0 \quad \text{for all } (i,j)\notin L, \tag{22c}$$

where H_{ij}^* is the complex conjugate of H_{ij}.

Proposition 1. *For the inner minimization problem of* (21)*, we have*

$$\inf_{v\in\mathbb{C}^{|N|}} v^* H(\pi) v = \begin{cases} 0 & \Lambda_{min}(\pi) \geq 0 \\ -\infty & \Lambda_{min}(\pi) < 0, \end{cases}$$

where $\Lambda_{min}(\pi)$ *is the smallest eigenvalue of* $H(\pi)$ *for any given* π*.*

Proof. Note that the Hermitian matrix $H(\pi)$ has real eigenvalues for any given π. Where $\Lambda_{min}(\pi) < 0$, there is an eigenvector v of $H(\pi)$ with a negative eigenvalue that specifies a direction of unbounded descent toward $-\infty$, and so the infimum of $-\infty$ is evident. Otherwise, for $\Lambda_{min}(\pi) \geq 0$, $H(\pi)$ is positive semidefinite, and the infimum is realized with value 0 by taking, for example, $v = 0$. □

Hence, the minimization problem is viewed as an indicator function for the constraint $\eta(\pi) \geq 0$ where

$$\eta(\pi) := \min_{v\in\mathbb{C}^{|N|}} \left\{ v^* H(\pi) v : \|v\|_2 \leq 1 \right\}, \tag{23}$$

which is a quadratic trust-region subproblem for which finding an optimal solution corresponds to finding an eigenvector of $H(\pi)$ of minimum eigenvalue. In the sequel, we work with the following concave, nonsmooth dual problem:

$$\begin{aligned} \Phi_D^{AC} = \max_{x,\pi} \; & \sum_{i\in N} \left[\alpha_i P_i^D + \beta_i Q_i^D - \gamma_i^+ (V_i^{max})^2 + \gamma_i^- (V_i^{min})^2 \right] && \text{(24a)} \\ & + \sum_{i\in N} \left[-\delta_i^{p,+} P_i^{max} + \delta_i^{p,-} P_i^{min} - \delta_i^{q,+} Q_i^{max} + \delta_i^{q,-} Q_i^{min} \right] \\ \text{s.t.} \; & \sum_{l\in L} x_l \leq K, \quad x_l \in \{0,1\}, \quad l \in L, \quad (x,\pi) \in \Pi && \text{(24b)} \\ & \eta(\pi) \geq 0. && \text{(24c)} \end{aligned}$$

3 Analysis of the Lagrangian Dual Bound of the Lower-Level Problem

We analyze the dual bound obtained by the Lagrangian relaxation of the lower-level problem ϕ^{AC}. In particular, we compare the Lagrangian dual bound with those from the SDP and SOC relaxations of the underlying ACOPF. In addition, we introduce a relaxation of the power flows (11), which exploits the power system network topology and physics. This structured relaxation can be applied to the SDP and SOC relaxations as well as the ACOPF subproblem.

3.1 SDP Relaxation of the Lower-Level Problem

We present the SDP relaxation of $\phi^{AC}(x)$ that can be obtained by replacing constraint (12b) by the SDP constraint $W \succeq 0$ (e.g., [BWFW08, LL12]), as follows:

$$\phi^{SDP}(x) := \min_{W,p^G,q^G,u} \left\{ \sum_{i\in N} (u_i^p + u_i^q + u_i^m) \text{ s.t. } W \succeq 0, \text{ (12c)} - \text{(12g)} \right\}. \tag{25}$$

Taking the Lagrangian relaxation of $\phi^{SDP}(x)$ with respect to constraints (12d)–(12g) as in (21), the SDP-based single-level reformulation is given by

$$\begin{aligned} \Phi_D^{SDP} := \max_{x,\pi} \; & \sum_{i\in N} \left[\alpha_i P_i^D + \beta_i Q_i^D - \gamma_i^+ (V_i^{max})^2 + \gamma_i^- (V_i^{min})^2 \right] && \text{(26)} \\ & + \sum_{i\in N} \left[-\delta_i^{p,+} P_i^{max} + \delta_i^{p,-} P_i^{min} - \delta_i^{q,+} Q_i^{max} + \delta_i^{q,-} Q_i^{min} \right] \\ & + \inf_W \left\{ \langle H(\pi), W \rangle \text{ s.t. } W \succeq 0 \right\} \\ \text{s.t.} \; & \sum_{l\in L} x_l \leq K, \quad x_l \in \{0,1\}, \quad l \in L, \quad (x,\pi) \in \Pi, \end{aligned}$$

where $\langle \cdot, \cdot \rangle$ is the Frobenius inner product over Hermitian matrices and $H(\pi)$ is given in (22). In the following proposition we show that $\Phi_D^{AC} = \Phi_D^{SDP}$ In words, the Lagrangian dual bound Φ_D^{AC} is as strong as the Lagrangian dual bound Φ_D^{SDP} while the computations of the two bounds are distinct.

Proposition 2. *The following equalities hold:*

$$\inf_v \{v^* H(\pi) v\} = \inf_{v,W} \{\langle H(\pi), W\rangle \text{ s.t. } W = v^* v\} = \inf_W \{\langle H(\pi), W\rangle \text{ s.t. } W \succeq 0\}.$$

Thus, problems (21) *and* (28) *are equivalent, and*

$$\Phi_D^{AC} = \Phi_D^{SDP}. \tag{27}$$

Proof. The first equality is straightforward. To verify the second equality, we start by defining the sets

$$\mathcal{W}^{AC} := \{W \in \mathbb{C}^{|N|\times|N|} : W = vv^* \text{ for some } v \in \mathbb{C}^{|N|}\}$$

and

$$\mathcal{W}^{SDP} := \{W : W \succeq 0\}.$$

Since the objective $\langle H(\pi), W\rangle$ is linear, we need only to show that $\text{conv}(\mathcal{W}^{AC}) = \mathcal{W}^{SDP}$. Noting that

$$\mathcal{W}^{AC} = \{W : W \in \mathcal{W}^{SDP} \text{ and } \text{rank}(W) = 1\},$$

we have that $\mathcal{W}^{AC} \subseteq \mathcal{W}^{SDP}$. The set $\mathcal{W}^{SDP}$ is also convex; and by the characterization of the convex hull being the smallest convex set containing a set, we have also

$$\mathcal{W}^{AC} \subset \text{conv}(\mathcal{W}^{AC}) = \text{cone}(\mathcal{W}^{AC}) \subseteq \mathcal{W}^{SDP},$$

where the middle equality holds since $\mathcal{W}^{AC}$ is a pointed convex cone. We show that in fact $\text{cone}(\mathcal{W}^{AC}) = \mathcal{W}^{SDP}$, by appealing to the characterization of a conic hull of a set as all finite conic combinations of elements in the set

$$\text{cone}(\mathcal{W}^{AC}) = \{\sum_{k=1}^{m} a_k W^k : m \in \mathbb{Z}^{++},\ W^k \in \mathcal{W}^{AC}, a_k \geq 0\ k = 1, \ldots, m\}.$$

In terms of matrices, and using the definition of $\mathcal{W}^{AC}$, we have

$$\text{cone}(\mathcal{W}^{AC}) = \left\{ \begin{array}{c} \sum_{k=1}^m a_k (v^k)(v^k)^* : m \in \mathbb{Z}^{++} \\ v^k \in \mathbb{C}^{|N|\times 1} \text{ are column vectors of complex bus voltages} \\ a_k \geq 0,\ k = 1, \ldots, m \end{array} \right\}.$$

Note that each $W^k := (v^k)(v^k)^*$ is a complex rank 1 $|N| \times |N|$ matrix. Each $W \in \mathcal{W}^{SDP}$ can be diagonalized with $|N|$ complex mutually orthonormal eigenvectors $v^1, \ldots, v^{|N|} \in \mathbb{C}^{|N|}$ with real nonnegative eigenvalues $0 \leq \nu_1 \leq \cdots \leq \nu_{|N|}$. One can easily verify from the diagonalization that $W = \sum_{k=1}^n \nu_k (v^k)(v^k)^*$. Thus, $W \in \text{cone}(\mathcal{W}^{AC})$, so that $\mathcal{W}^{SDP} = \text{cone}(\mathcal{W}^{AC})$ has been established. □

The inner minimization of (26) implies the dual feasibility requirement that $H(\pi) \succeq 0$ (see, e.g., [Hel02, Theorem 2.4(4)]), and so (26) can also be written as

$$\begin{aligned} \Phi_D^{SDP} = \max_{x,\pi} \quad & \sum_{i\in N} \left[\alpha_i P_i^D + \beta_i Q_i^D - \gamma_i^+ (V_i^{max})^2 + \gamma_i^- (V_i^{min})^2\right] \\ & + \sum_{i\in N} \left[-\delta_i^{p,+} P_i^{max} + \delta_i^{p,-} P_i^{min} - \delta_i^{q,+} Q_i^{max} + \delta_i^{q,-} Q_i^{min}\right] \\ \text{s.t.} \quad & \sum_{l\in L} x_l \leq K, \quad x_l \in \{0,1\}, \quad l \in L, \quad (x,\pi) \in \Pi, \quad H(\pi) \succeq 0. \end{aligned} \tag{28}$$

Note that although $H(\pi)$ is given as a complex matrix, its translation into a form that is suitable for a modeling language is straightforward, where $H(\pi) \succeq 0$ is equivalent to

$$\left[\begin{array}{cc} \Re\{H(\pi)\} & \Im\{H(\pi)\} \\ \Im\{H(\pi)\} & \Re\{H(\pi)\} \end{array} \right] \succeq 0. \tag{29}$$

3.2 SOC Relaxation of the Lower-Level Problem

It is also well known that the SOC relaxation of $\phi^{SDP}(x)$ is obtained by replacing the SDP constraint with a second-order cone constraint as follows:

$$\begin{aligned}\phi^{SOC}(x) := \min_{W,p^G,q^G,u} \quad & \sum_{i\in N}(u_i^p + u_i^q + u_i^m) \\ \text{s.t.} \quad & \left\| \begin{array}{c} 0.5(W_{ii} - W_{jj}) \\ W_{ij}^R \\ W_{ij}^I \end{array} \right\|_2 \leq 0.5(W_{ii} + W_{jj}),\ (i,j) = l \in L \\ & \text{(12c)} - \text{(12g)}.\end{aligned} \tag{30}$$

Following the analogous development from (30) as done in Sections 2.2 and 3.1 and applying the SOC duality theory, we obtain the following SOC dual problem:

$$\begin{aligned}\Phi_D^{SOC} := \max_{\substack{x,\pi,\xi \\ \nu,\omega}} \ & \sum_{i\in N}\left[\alpha_i P_i^D + \beta_i Q_i^D - \gamma_i^+ (V_i^{max})^2 + \gamma_i^- (V_i^{min})^2\right] \\ & + \sum_{i\in N}\left[-\delta_i^{p,+} P_i^{max} + \delta_i^{p,-} P_i^{min} - \delta_i^{q,+} Q_i^{max} + \delta_i^{q,-} Q_i^{min}\right] \\ \text{s.t.} \ & \sum_{l\in L} x_l \leq K, \quad x_l \in \{0,1\}, \quad l \in L \\ & H_{ii}(\pi) + 0.5\sum_{l\in L_i^f}(\xi_l^D - \nu_l) - 0.5\sum_{l\in L_i^t}(\xi_l^D + \nu_l) - \omega_i = 0, \quad i \in N \\ & 2H_{ij}^R(\pi) + \xi_l^R = 0, \qquad 2H_{ij}^I(\pi) + \xi_l^I = 0, \quad l \in L \\ & \left\| \begin{array}{c} \xi_l^D \\ \xi_l^R \\ \xi_l^I \end{array} \right\| \leq \nu_l, \quad l \in L \\ & (x,\pi) \in \Pi, \quad \nu_l \geq 0, \quad l \in L, \quad \omega_i \geq 0, \quad i \in N.\end{aligned} \tag{31}$$

The formulation (31) is similar to the one developed in [WCA18] except that the corresponding formulation in [WCA18] also accounts for line flow bounds in the defender subproblem, which we relax in all formulations.

3.3 A Structured Relaxation of the Power Flows Equations

We introduce a new relaxation to the defender subproblem (12), whose formulation is obtained with the addition of auxiliary variables

$$h := (h_l^{p,f}, h_l^{p,t}, h_l^{q,f}, h_l^{q,t})_{l\in L} \in \mathcal{H} \subset \mathbb{R}^{4|L|}$$

to the corresponding line flow values in (8). We assume that set $\mathcal{H}$ has a linear subspace structure. This corresponds to altering the net power injections (9) as follows:

$$p_i^H(W,x,h) := p_i^N(W,x) + \sum_{l\in L_i^f}(1-x_l)h_l^{p,f} + \sum_{l\in L_i^t}(1-x_l)h_l^{p,t}, \tag{32a}$$

$$q_i^H(W,x,h) := q_i^N(W,x) + \sum_{l\in L_i^f}(1-x_l)h_l^{q,f} + \sum_{l\in L_i^t}(1-x_l)h_l^{q,t}. \tag{32b}$$

Consequently, we consider the lower-level problem of the form

$$\begin{aligned}\phi_{\mathcal{H}}^{AC}(x) := \min_{v,W,p^G,q^G,u,h} \quad & \sum_{i\in N}(u_i^p + u_i^q + u_i^m) \\ \text{s.t.} \quad & \text{(12b)} - \text{(12d)}, \text{(12g)}, \qquad h \in \mathcal{H} \\ & -u_i^p \leq p_i^H(W,x,h) - p_i^G + P_i^D \leq u_i^p, \qquad i \in N, \\ & -u_i^q \leq q_i^H(W,x,h) - q_i^G + Q_i^D \leq u_i^q, \qquad i \in N.\end{aligned} \tag{33}$$

The dual single-level problem analogous to (24) is given by

$$\Phi^{AC}_{D,\mathcal{H}} := \max_{x,\pi} \quad \sum_{i\in N}\left[\alpha_i P_i^D + \beta_i Q_i^D - \gamma_i^+ (V_i^{max})^2 + \gamma_i^- (V_i^{min})^2\right] \tag{34a}$$

$$+ \sum_{i\in N}\left[-\delta_i^{p,+} P_i^{max} + \delta_i^{p,-} P_i^{min} - \delta_i^{q,+} Q_i^{max} + \delta_i^{q,-} Q_i^{min}\right]$$

$$\text{s.t.} \sum_{l\in L} x_l \le K, \quad x_l \in \{0,1\},\ l \in L, \quad (x,\pi)\in\Pi, \quad 0 \le \eta(\pi) \tag{34b}$$

$$(\lambda^f, \lambda^t, \mu^f, \mu^t) \in \mathcal{H}^\perp, \tag{34c}$$

where $\mathcal{H}^\perp$ is the orthogonal complement to the subspace $\mathcal{H}$. The constraint (34c) is necessary for dual feasibility and the subsequent vanishing of the h terms in the Lagrangian.

For SDP, we analogously obtain

$$\phi^{SDP}_{\mathcal{H}}(x) := \min_{v,W,p^G,q^G,u,h} \quad \sum_{i\in N}(u_i^p + u_i^q + u_i^m) \tag{35}$$

$$\begin{aligned}
\text{s.t.}\quad & W \succeq 0, \qquad u^p, q^q, u^m \in \mathbb{R}^{|N|}_+, \qquad h \in \mathcal{H}\\
& P_i^{min} \le p_i^G \le P_i^{max}, \quad Q_i^{min} \le q_i^G \le Q_i^{max}, \quad i \in N\\
& -u_i^p \le p_i^H(W,x,h) - p_i^G + P_i^D \le u_i^p, \qquad i \in N\\
& -u_i^q \le q_i^H(W,x,h) - q_i^G + Q_i^D \le u_i^q, \qquad i \in N\\
& (V_i^{min})^2 - u_i^m \le W_{ii} \le (V_i^{max})^2 + u_i^m, \qquad i \in N
\end{aligned}$$

and

$$\Phi^{SDP}_{D,\mathcal{H}} := \max_{x,\pi} \quad \sum_{i\in N}\left[\alpha_i P_i^D + \beta_i Q_i^D - \gamma_i^+ (V_i^{max})^2 + \gamma_i^- (V_i^{min})^2\right] \tag{36a}$$

$$+ \sum_{i\in N}\left[-\delta_i^{p,+} P_i^{max} + \delta_i^{p,-} P_i^{min} - \delta_i^{q,+} Q_i^{max} + \delta_i^{q,-} Q_i^{min}\right]$$

$$\text{s.t.} \sum_{l\in L} x_l \le K, \quad x_l \in \{0,1\}, \quad l \in L, \quad (x,\pi)\in\Pi \tag{36b}$$

$$H(\pi) \succeq 0, \qquad (\lambda^f, \lambda^t, \mu^f, \mu^t) \in \mathcal{H}^\perp.$$

Furthermore, Proposition 2 implies the following corollary.

Corollary 1. *For a given linear subspace $\mathcal{H} \subset \mathbb{R}^{4|L|}$, both problems* (34) *and* (36) *have the same optimal value; that is,*

$$\Phi^{AC}_{D,\mathcal{H}} = \Phi^{SDP}_{D,\mathcal{H}}. \tag{37}$$

We now introduce a structured relaxation of the nodal power balance by defining an instance of the linear subspace $\mathcal{H}$ as follows:

$$\mathcal{H} := \left\{ \begin{array}{c} \left(h^{p,f}, h^{p,t}, h^{q,f}, h^{q,t}\right) : \\ h_l^{p,f} = -h_l^{p,t}, \quad h_l^{q,f} = -h_l^{q,t}, \quad l \in L \end{array} \right\}. \tag{38}$$

The relaxation is partial and structured, because this manner of controlling $h \in \mathcal{H}$ allows for the free, but balanced, exchange of power between two connected buses $i, j \in N$ by line $(i,j) = l \in L$ while *preserving the network topology* under contingency. The exchange is free in the sense that it is not restricted by the bus voltage settings as would normally be the case in AC power flow due to (6).

For $\mathcal{H}$ as given in (38), the dual feasibility constraint (34c) takes the form

$$(\lambda^f, \lambda^t, \mu^f, \mu^t) \in \mathcal{H}^\perp = \left\{ \begin{array}{c} \left(\lambda_l^f, \lambda_l^t, \mu_l^f, \mu_l^t\right)_{l\in L} : \\ \lambda_l^f = \lambda_l^t, \quad \mu_l^f = \mu_l^t \quad l \in L \end{array} \right\}. \tag{39}$$

Note that this relaxation can be applied to $\phi^{AC}(x), \phi^{SDP}(x)$, and $\phi^{SOC}(x)$ in addition to the relaxations to the rank 1 power flow constraints (12b).

3.4 Relationships Between the Relaxations

We have shown that $\Phi_D^{SDP} = \Phi_D^{AC}$ and $\Phi_{D,\mathcal{H}}^{SDP} = \Phi_{D,\mathcal{H}}^{AC}$, respectively, from Propositions 2 and 1. Recall that we denote by Φ^{AC}, Φ^{SDP}, and Φ^{SOC}, respectively, the optimal objective value of (1) with $\phi = \phi^{AC}(x)$, $\phi^{SDP}(x)$, and $\phi^{SOC}(x)$. The following proposition is immediate from the well-known relations of the SDP and SOC relaxations of ACOPF.

Proposition 3. $\Phi^{AC} \geq \Phi^{SDP} \geq \Phi^{SOC}$.

Proof. It is derived from the relations $\phi^{AC}(x) \geq \phi^{SDP}(x) \geq \phi^{SOC}(x)$ for any x (e.g., [CHH16]). □

In addition, we show that the strong duality holds for each relaxation in the following proposition.

Proposition 4. *The relaxations* (25), (30), *and* (35) *satisfy Slater's condition. Consequently, we have*

$$\Phi_D^{SOC} = \Phi^{SOC}, \quad \Phi_D^{SDP} = \Phi^{SDP}, \quad \textit{and} \quad \Phi_{D,\mathcal{H}}^{SDP} = \Phi_{\mathcal{H}}^{SDP}.$$

Proof. We verify the satisfaction of Slater's condition by setting

$$W_{ii} = 1, \quad i \in N, \quad W_{ij} = 0, \quad i \neq j \in N$$
$$p_i^G = \frac{P_i^{max} - P_i^{min}}{2}, \quad q_i^G = \frac{Q_i^{max} - Q_i^{min}}{2} \quad i \in N$$

and choosing $u_i^p > 0,\ u_i^q > 0,\ u_i^m > 0$ such that

$$-u_i^p < p_i^N(W,x) - p_i^G + P_i^D < u_i^p, \quad -u_i^q < q_i^N(W,x) - q_i^G + Q_i^D < u_i^q, \quad i \in N$$
$$(V_i^{min})^2 - u_i^m < W_{ii} < (V_i^{max})^2 + u_i^m, \quad i \in N,$$

and in the case of (35), additionally setting $h = 0$. W is set to the identity matrix, so clearly $W \succ 0$. □

Note that the weak duality $\Phi_D^{AC} \leq \Phi^{AC}$ and $\Phi_{D,\mathcal{H}}^{AC} \leq \Phi_{\mathcal{H}}^{AC}$ also hold. Thus, from the reasoning of this subsection and from Proposition 4, we conclude this section with the following proposition.

Proposition 5. *The following chains of relations hold:*

1. $\Phi_D^{SOC} = \Phi^{SOC} \leq \Phi_D^{SDP} = \Phi^{SDP} = \Phi_D^{AC} \leq \Phi^{AC}$
2. $\Phi_{D,\mathcal{H}}^{SDP} = \Phi_{\mathcal{H}}^{SDP} = \Phi_{D,\mathcal{H}}^{AC} \leq \Phi_D^{SDP} = \Phi^{SDP} = \Phi_D^{AC}$
3. $\Phi_{D,\mathcal{H}}^{SDP} = \Phi_{\mathcal{H}}^{SDP} = \Phi_{D,\mathcal{H}}^{AC} \leq \Phi_{\mathcal{H}}^{AC}$.

No relationship between $\Phi_{\mathcal{H}}^{SDP}$ and Φ^{SOC} or between $\Phi_{D,\mathcal{H}}^{SDP}$ and Φ_D^{SOC} is evident.

4 Algorithms and Methods

In this section, we present the single-tree extended cutting plane (1T-ECP) algorithm for solving the Lagrangian dual problems (24) and (34), and we provide an analysis of convergence. The algorithm is a variant of the ECP algorithm [WP95b], which adds the cutting planes at each integer feasible solution *within one branch-and-cut tree*, whereas the ECP algorithm solves a mixed-integer nonlinear program for each cutting plane that is added (i.e., solving over multiple branch-and-cut trees). This single-tree aspect also appears in the approach of [QG92], where each node subproblem is a nonlinear program.

4.1 Single-Tree Extended Cutting Plane Algorithm

We describe the 1T-ECP algorithm for problem of the form

$$\max_y \{\theta(y) : g_A(y) \leq 0,\ g_N(y) \leq 0\}, \tag{40}$$

where $\theta : \mathbb{R}^{n_R} \times \{0,1\}^{n_I} \mapsto \mathbb{R}$ is an affine function; $g_A : \mathbb{R}^{n_R} \times \{0,1\}^{n_I} \mapsto \mathbb{R}^{m_A}$ define affine constraints; and $g_N : \mathbb{R}^{n_R} \times \{0,1\}^{n_I} \mapsto \mathbb{R}$ is a nonsmooth, nonlinear, and convex function. For convenience, we write $y = (y_R, y_I)$ when distingushing between the continuous (y_R) and integer-restricted (y_I) components of y. We assume that (40) is feasible and that the set $\{y : g_A(y) \leq 0\}$ is bounded, implying the boundedness of (40).

For the sake of nontriviality, we assume that g_N cannot be written as the supremum or infimum of a finite number of differentiable functions. Within the cutting plane methodology, we iteratively add linear inequalities to lower-approximate the function g_N using information including function values $g_N(y^j)$ and subgradients $s^j \in \partial(y^j)$ generated during the iterations $j = 0, \ldots, k$.

Next, we introduce the notation for the branch-and-cut process in the 1T-ECP algorithm. Let $\mathcal{T}$ be a branch-and-cut tree that consists of a set of tree nodes $\mathcal{N}$ solved in the 1T-ECP algorithm, and let C^k be the set of indices for the linear inequalities added to lower-approximate the function g_N at iteration k. At each tree node $\mathcal{N} \in \mathcal{T}$, the algorithm may fix some of the binary variables y_I to either 0 or 1 as part of the branching process. We denote by $\mathcal{B}_0^{\mathcal{N}}$ the set of indices of y_I components that are fixed to 0 at node $\mathcal{N}$, and we denote by $\mathcal{B}_1^{\mathcal{N}}$ the set of indices of y_I components that are fixed to 1 at node $\mathcal{N}$. The upper bound associated with each node is $\theta_{UB}^{\mathcal{N}}$, and the incumbent lower bound associated with the best-known feasible solution is θ_{LB}. We now define $B^{\mathcal{N}}$ for a given node $\mathcal{N}$ as

$$B^{\mathcal{N}} := \left\{ y_I \in [0,1]^{n_I} : y_{I,i} = 0\ \forall i \in \mathcal{B}_0^{\mathcal{N}},\ y_{I,i} = 1\ \forall i \in \mathcal{B}_1^{\mathcal{N}} \right\},$$

The 1T-ECP algorithm solves the following node subproblem at node $\mathcal{N}$ at iteration k,

$$\begin{aligned} \theta^{\mathcal{N}} = \max_y \quad & \theta(y) \\ \text{s.t. } & g_A(y) \leq 0, \qquad y_I \in B^{\mathcal{N}} && \text{(41a)} \\ & g_N(y^c) + (s^c)^\top (y - y^c) \leq 0 \quad \forall c \in C^k, && \text{(41b)} \end{aligned}$$

where $s^c \in \partial\theta(y^c)$. We emphasize that all cuts of the form (41b) are valid for any tree node $\mathcal{N} \in \mathcal{T}$ and for (40).

1T-ECP is summarized in Algorithm 1. The algorithm initializes the branch-and-cut tree $\mathcal{T}$, the index set C^k for cutting planes, and the iteration counter k (line 1). The root node is created (line 2) and added to the tree $\mathcal{T}$ (line 3). At each node, the inner node processing loop repeats whenever any cuts are added (line 21). The outer loop runs until no tree node exists in $\mathcal{T}$ (lines 4 – 37). Note that one can easily add additional criteria such as time limit and node limit.

The inner loop of lines 9–35 terminates if one of the following three criteria is satisfied:

1. Fathoming due to either bound or infeasibility at line 15
2. Branching on a fractional variable value y^{k+1} at lines 28–32
3. After updating the node subproblem solution y^{k+1} at line 10, it is verified that

$$g_N(y^{k+1}) \leq \epsilon, \text{ and } y_I^{k+1} \in \{0,1\}^{n_I}, \tag{42}$$

that is, y^{k+1} is feasible to (40) (with tolerance ϵ), and feasible (with tolerance ϵ) and optimal for the node $\mathcal{N}$ subproblem (41) (line 26), in which case, node $\mathcal{N}$ is fathomed by optimality, and, as appropriate, incumbent solution and value are updated.

We show that the inner loop at lines 9–35 must terminate after finitely many iterations for feasibility tolerance $\epsilon > 0$.

Lemma 1. *Let $\epsilon > 0$, and let $\mathcal{N} \in \mathcal{T}$ be a node whose processing reaches the inner loop of lines 9–35. Then after a finite number of inner loop iterations (lines 9–35), the processing of node $\mathcal{N}$ must finish because of one of the following three criteria:*

Algorithm 1 Single-tree extended cutting plane algorithm applied to (40)

Initialize $\mathcal{T} \leftarrow \emptyset$, $k \leftarrow 0$, $C^k \leftarrow \emptyset$, $\epsilon \geq 0$, $\theta_{LB} \leftarrow -\infty$, $y^{LB} \leftarrow y^0$
Create a root node $\mathcal{N}$ such that $\mathcal{B}_0^{\mathcal{N}} \leftarrow \emptyset$, $\mathcal{B}_1^{\mathcal{N}} \leftarrow \emptyset$, and $\theta_{UB}^{\mathcal{N}} \leftarrow \infty$
Set $\mathcal{T} \leftarrow \{\mathcal{N}\}$
while $\mathcal{T} \neq \emptyset$ **do**
  Choose a node $\mathcal{N} \in \mathcal{T}$, and update $\mathcal{T} \leftarrow \mathcal{T} \backslash \{\mathcal{N}\}$
  if $\theta_{UB}^{\mathcal{N}} \leq \theta_{LB}$ **then**
    Fathom node $\mathcal{N}$ due to bound and set $C^{k+1} \leftarrow C^k$
  else
    repeat
      Solve the node subproblem (41)
      If (41) is optimally solved, let y^{k+1} be an optimal solution
          and set $\theta_{UB}^{\mathcal{N}}$ to the optimal value
      Set cutNotAdded $\leftarrow$ **true**.
      if node subproblem (41) is infeasible or $\theta_{UB}^{\mathcal{N}} \leq \theta_{LB}$ **then**
        Set $C^{k+1} \leftarrow C^k$ {fathom due to infeasibility or bound}
      else
        if $y_I^{k+1} \in \{0,1\}^{n_I}$ **then**
          if $g_N(y^{k+1}) > \epsilon$ **then**
            Compute subgradient $s^{k+1} \in \partial g_N(y^{k+1})$ for adding a cut of form (41b)
            Update $C^{k+1} \leftarrow C^k \cup \{k+1\}$
            cutNotAdded $\leftarrow$ **false**
          else
            if $\theta_{UB}^{\mathcal{N}} > \theta_{LB}$ **then**
              $\theta_{LB} \leftarrow \theta_{UB}^{\mathcal{N}}$, $y^{LB} \leftarrow y^{k+1}$ {update incumbent solution and value}
            end if
            Set $C^{k+1} \leftarrow C^k$ {fathom due to optimality}
          end if
        else
          Choose some index i such that $y_{I,i}^{k+1} \notin \{0,1\}$.
          Create two nodes $\mathcal{N}_0$ and $\mathcal{N}_1$ such that

$$1.\quad \mathcal{B}_0^{\mathcal{N}_0} \leftarrow \mathcal{B}_0^{\mathcal{N}} \cup \{i\}, \quad \mathcal{B}_1^{\mathcal{N}_0} \leftarrow \mathcal{B}_1^{\mathcal{N}}, \quad \theta_{UB}^{\mathcal{N}_0} \leftarrow \theta_{UB}^{\mathcal{N}}$$
$$2.\quad \mathcal{B}_0^{\mathcal{N}_1} \leftarrow \mathcal{B}_0^{\mathcal{N}}, \quad \mathcal{B}_1^{\mathcal{N}_1} \leftarrow \mathcal{B}_1^{\mathcal{N}} \cup \{i\}, \quad \theta_{UB}^{\mathcal{N}_1} \leftarrow \theta_{UB}^{\mathcal{N}}$$

          Set $\mathcal{T} \leftarrow \mathcal{T} \cup \{\mathcal{N}_0, \mathcal{N}_1\}$ and $C^{k+1} \leftarrow C^k$ {Branching on $y_{I,i}^{k+1}$}
        end if
      end if
      Set $k \leftarrow k+1$
    until cutNotAdded
  end if
end while

1. *fathoming the node due to either bound or infeasibility at line 15;*

2. *fathoming the node due to optimality at line 26; or*

3. *branching on a fractional variable value y^{k+1} at line 31.*

Proof. Note that every iteration of the inner loop (lines 9–35) should visit line 15, line 21, line 26, or line 31. The inner loop terminates unless line 21 is visited at every inner loop iteration.

Suppose that at the given node $\mathcal{N} \in \mathcal{T}$, the inner loop of lines 9–35 infinitely visits line 21 only. Let $\{y^k\}_{k=1..\infty}$ be the sequence generated by this loop, and let $\bar{y}$ be an accumulation point. By the assumption, we have $g_A(y^k) \leq 0$ and $g_N(y^k) > \epsilon$, $k \geq 1$, for a given tolerance $\epsilon > 0$. Also, the continuity of g_A and g_N implies that $g_A(\bar{y}) \leq 0$ and $g_N(\bar{y}) \geq \epsilon$. Let $\delta > 0$ be small enough that a local Lipschitz condition with constant L holds for g_N in the ball $B(\bar{y}, \delta) := \{y : \|y - \bar{y}\|_2 \leq \delta\}$. Denote $\hat{\epsilon} = \min\{\frac{\epsilon}{3L}, \delta\}$. Since $\bar{y}$ is an accumulation point, there exist indices $k > j$ such that $y^j, y^k \in B(\bar{y}, \hat{\epsilon})$ for the node subproblem solutions y^j and y^k, respectively, at iterations j and k. Since $k > j$, we have the satisfaction of the (41b) inequality

$$g_N(y^j) + (s^j)^T(y^k - y^j) \leq 0,$$

and thus the inequalities

$$\begin{aligned} \epsilon \leq g_N(\bar{y}) &\leq |g_N(\bar{y}) - g_N(y^j) - (s^j)^T(y^k - y^j)| && \text{(43a)} \\ &\leq |g_N(\bar{y}) - g_N(y^j)| + \|s^j\|\|y^k - y^j\| && \text{(43b)} \\ &\leq L\|\bar{y} - y^j\| + L\|y^k - \bar{y}\| + L\|\bar{y} - y^j\| && \text{(43c)} \end{aligned}$$

also hold, where the inequalities (43b) and (43c) hold due to the Cauchy-Schwartz inequality and the Lipschitz continuity, respectively. Moreover, because of $y^j, y^k \in B(\bar{y}, \hat{\epsilon})$, we have

$$L\|\bar{y} - y^j\| + L\|y^k - \bar{y}\| + L\|\bar{y} - y^j\| < \epsilon$$

and thus $g_N(\bar{y}) < \epsilon$, which contradicts the assumption. Therefore, the inner loop should visit line 15, line 26, or line 31 after a finite number of visits to line 21. □

We now show the finite termination of Algorithm 1 with a global optimal solution of problem (40).

Theorem 1. *For any feasibility tolerance $\epsilon > 0$, Algorithm 1 applied to any feasible instance of problem* (40) *terminates with a globally optimal solution for problem* (40).

Proof. Algorithm 1 processes a finite number of nodes, and each node subproblem is guaranteed to be processed within a finite number of iterations of the inner loop of lines 9–35 because of infeasibility, bound, or optimality (by Lemma 1). (The application of Lemma 1 is needed only for those nodes that are not immediately fathomed due to bound at line 7.) Since problem (40) is feasible by assumption, there must be at least one node processed to optimality. Of these nodes, at least one must have been identified as having a globally optimal solution. □

4.2 Methods for Solving Relaxations of Problem (1)

Although problem (23) is nonconvex, its quadratic trust-region subproblem structure guarantees that a globally optimal solution can be found. Recall that $H(\pi)$ is defined in (22).

Proposition 6. *If, for fixed π, $H(\pi)$ is positive semidefinite, then $v = 0$ is an optimal solution to problem* (23). *Otherwise, if $H(\pi)$ has at least one negative eigenvalue, then a global optimal solution of* (23) *is given by any eigenvector of $H(\pi)$ associated with the minimal eigenvalue.*

Proof. This is a well-known result for quadratic trust-region subproblems. See, for example, [Hag01, GLRT99]. □

Furthermore, the following proposition derives subgradients $\sigma \in \partial\eta(\pi)$ of the function (23).

Proposition 7. *The value function η defined in* (23) *is concave. Given an optimal solution $\hat{v}$ to problem* (23) *with $\pi = \pi^* \in \mathbb{R}^{8|N|+4|L|}$, subgradients $\sigma_\pi \in \partial\eta(\pi^*)$ are given by*

$$\sigma_{\alpha,i} = p_i^{sh}(\widehat{W}_{ii}),\ \sigma_{\beta,i} = q_i^{sh}(\widehat{W}_{ii}),\ \sigma_{\gamma^-,i} = -\widehat{W}_{ii},\ \sigma_{\gamma^+,i} = \widehat{W}_{ii} \quad \forall i \in N \tag{44a}$$

$$\sigma_{\lambda^f,l} = p_l^f(\widehat{W}_l),\ \sigma_{\lambda^t,l} = p_l^t(\widehat{W}_l),\ \sigma_{\mu^f,l} = q_l^f(\widehat{W}_l),\ \sigma_{\mu^t,l} = q_l^t(\widehat{W}_l), \quad \forall l \in L, \tag{44b}$$

where we set $\widehat{W} = \hat{v}\hat{v}^*$.

Proof. The feasible set in problem (23) is compact; its objective function is continuous in v and linear in π. From [Cla90, Corollary 1 of Section 2.8], $\pi \mapsto \eta(\pi)$ is concave, and $\sigma_\pi \in \partial\eta(\pi^*)$. □

Thus, the applications of Algorithm 1 to problem (1) via formulations (24) and (34) are implementable.

5 Computational Experiments

In this section, we present computational experiments by applying Algorithm 1 to (24) and (34). In particular, we call the method of applying Algorithm 1 to (24) 1T-ECP-AC and call the method of applying Algorithm 1 to (34) 1T-ECP-R. Moreover, we call the methods for solving the SDP and SOC relaxations (28) and (31) with known algorithms miSDP and miSOC, respectively. Note that miSOC is similar to the method developed in [WCA18] except that the formulation in [WCA18] also accounts for line flow bounds, which we relax in all of our formulations. We report the computational performance of the four methods: 1T-ECP-AC, 1T-ECP-R, miSDP, and miSOC. The methods were run with the time limit of 24 wall-clock hours (86,400 seconds).

5.1 Test Instances

The test problem instances include the IEEE 30-, 57-, 118-, and 300-bus test systems and Pegase 1354-, and 2869-bus systems [oWDoEE99]. For each test case, we consider attack budgets $K \in \{1, 2, 3, 4\}$. Table 1 provides a profile of the number of components for each test case.

Table 1: Data associated with each of the test problems.

Number of Components by Type		IEEE Case				Pegase Case	
Type	Index Set	30	57	118	300	1354	2869
Buses	N	30	57	118	300	1354	2869
Generators	G	6	7	54	69	260	510
Loads (fixed)		20	42	99	201	673	1491
Shunts		2	3	14	29	1082	2197
Branches	L	41	80	186	411	1991	4582
Transformers		0	17	9	107	234	496

5.2 Implementation

The modeling and solver parameterizations for the tests of the methods 1T-ECP-AC, 1T-ECP-R, miSDP, and miSOC are implemented in Julia 0.6, using the JuMP [DHL17] modeling interface. CPLEX 12.7 [IBM] is used as the solver for the master problem updates (41) for the 1T-ECP-AC and 1T-ECP-R methods, where the mixed-integer linear problem instances are solved by CPLEX with lazy constraints added via callback to approximate the value function η defined in (23). This callback is invoked whenever an integer-feasible solution is encountered anywhere in the search tree. CPLEX parameterizations are nearly default, except that we modified the `purgeable` option in `setcallbackcut` method, as invoked in the `cblazy` method in `cpx_callbacks.jl`, to take the value `CPX_USECUT_PURGE`. The subproblems (23), corresponding to eigenvalue minimization problems, are solved with the Julia LinearAlgebra `eigs` function with nondefault arguments `which=:SR`, `maxiter=100000`, and `tol=1e-8`.

For the miSDP method tests, Mosek [MOS19] is used to solve the continuous SDP relaxations, while a simple branch-and-bound framework is implemented by using Julia JuMP. In particular, node selection is

based on best bound, and the branching variable index is chosen by $\text{argmax}_l\{\min\{|1-x_l|, x_l\}(1+\|Y_l\|_F)\}$, where $\|\cdot\|_F$ is the Frobenius norm on the 2×2 matrices Y_l, $l \in L$, which are defined in (3). We note that the SDP relaxation can potentially be improved by exploiting the sparsity structure (e.g., chordal graph [ZFP+17, MHLD13]), which is not implemented in our miSDP method. We do not use a primal heuristic to obtain incumbent bounds; we obtain only potential incumbent bounds when fathoming due to optimality occurs at a node. Since implementing such advanced algorithmic features is not the focus of this paper, we leave that as future work. Mosek has built-in support for solving mixed-integer SOC problems, and so Mosek is used to solve the instances in the tests of the miSOC method. Parameter settings for the use of Mosek are nearly default, except for enforcing the use of one thread.

Each of the computational tests is carried out on a single core of a single node of the Argonne National Laboratory Bebop cluster, each consisting of an Intel® Xeon® CPU E5-2695 v4 @ 2.10 GHz processor. We use the GNU `Parallel` utility [Tan11] in submitting jobs in parallel using one core per job. Appropriate parameters for enforcing the use of one thread are set either automatically (multithreading is disabled with the use of the lazy constraint callback feature of CPLEX) or explicitly in the instantiation of the Mosek solver object.

For all experiments, we report the following in Tables **??**:

1. number of nodes (Nodes);
2. average time (in seconds) spent solving each node (Secs/N);
3. total running time for solving the instance, in seconds (Secs);

Additionally, the following information about the lazy cuts is provided in Tables **??** for the 1T-ECP-AC and 1T-ECP-R method tests:

1. number of user cuts applied (Cuts) and
2. percentage of the total run time spent generating the lazy cuts (% Time).

Incumbent solutions x, incumbent objective values, and gaps between upper and lower bound values at termination are reported in Tables **??**. Furthermore, Figure 1 provides plots of ϕ^{SOC} values from Table 5 against the wall times from Table 4 obtained from the 1T-ECP-R and miSOC tests.

5.3 Comparison between 1T-ECP-AC and miSDP

Qualitatively, we may compare the 1T-ECP-AC and miSDP methods as follows. For method miSDP each node is processed by solving a continously relaxed SDP problem exactly, while for method 1T-ECP-AC each node is processed by solving a cutting plane approximation of the corresponding continously relaxed SDP subproblem, and improvements in this approximation are enforced only while the approximate solution is integer feasible. Consequently, we expect for larger problems that (1) the processing of each node usually takes less time in the 1T-ECP-AC test than in the miSDP test, but that (2) the node bounds in the miSDP tests are usually tighter in comparison with the corresponding node bounds computed in the 1T-ECP-AC tests.

In Table 2, we observe that the 1T-ECP-AC tests have always processed more nodes than the miSDP tests for the Case 118 instances have. On the other hand, processing each node takes much less time in 1T-ECP-AC than for miSDP, where the poor scalability of the SDP solver starts becoming evident. Times to generate cuts in the 1T-ECP-AC tests take smaller percentages of the total run time for larger instances. This result implies that most computational effort for the application of 1T-ECP-AC is in updating the master problem solution.

Table 3 reports the solutions found by the two methods. In the allotted time, the miSDP tests usually show a smaller gap between the upper and lower bound than for 1T-ECP-AC; also, the miSDP tests almost always produce solutions at least as good as, and often better than, those produced in the 1T-ECP-AC tests. The exception appears for the IEEE Case 118 test with $K = 4$, which fails to find an integer feasible solution because of the search tree not getting large enough to discover a node that is fathomed by optimality. Note that if we ignore numerical error, both methods should produce the same optimal values when termination due to convergence is achieved.

As a proof of concept, 1T-ECP-AC may be regarded as a potential alternative to miSDP, which requires the solutions of large SDP problems. The main bottleneck to the 1T-ECP-AC approach is the need to generate many cuts, thus increasing the time to process each node. Improvement may be found, for example,

Table 2: Computational performance of 1T-ECP-AC and miSDP for smaller test instances (IEEE 30-, 57-, 118-bus systems with $K = 1, 2, 3, 4$)

		1T-ECP-AC					miSDP		
Case	K	Cuts	% Time	Nodes	Secs/N	Secs	Nodes	Secs/N	Secs
30	1	3053	8.00	83	0.84	69	57	1.4	80
	2	4134	3.80	562	0.32	182	37	1.6	59
	3	6930	1.71	979	0.77	756	223	1.5	325
	4	8137	1.44	2608	0.62	1613	317	1.6	506
57	1	24747	0.58	118	230.61	27212	69	44.9	3094
	2	28238	0.41	592	67.28	39827	303	53.3	16149
	3	37619	0.33	1816	47.58	86400	1757	49.2	86400
	4	38521	0.33	1398	61.80	86400	2223	38.9	86400
118	1	14167	0.35	372	60.47	22495	5	2632.9	13164
	2	17656	0.15	12965	5.63	72981	35	2470.9	86400
	3	17939	0.13	12089	7.15	86400	22	3927.3	86400
	4	20727	0.14	4946	17.47	86400	20	4320.0	86400

Table 3: IEEE Case 30, 57, 118 tests: solutions, values, and gaps. Values of ϕ^{SDP} with $*$ superscript indicate possibly suboptimal values due to the test reaching the allotted time limit.

		1T-ECP-AC			miSDP		
Case	K	Lines Cut	ϕ^{SDP}	% Gap	Lines Cut	ϕ^{SDP}	% Gap
30	1	34	0.058	0.0	34	0.058	0.0
	2	10 40	0.600	0.0	10 40	0.600	0.0
	3	10 34 40	0.658	0.0	10 34 40	0.658	0.0
	4	8 9 10 40	0.937	0.0	8 9 10 40	0.937	0.0
57	1	41	0.372	0.0	41	0.368	0.0
	2	41 80	0.780	0.0	41 80	0.777	0.0
	3	28 33 41	0.623^*	440.3	33 41 80	1.024^*	7.9
	4	41 61 66 72	1.092^*	525.7	60 65 66 72	1.600^*	29.5
118	1	183	0.840	0.0	183	0.840	0.0
	2	121 125	1.448	0.0	121 125	1.448^*	4.7
	3	90 121 125	1.448^*	>1000.0	121 125 183	2.288^*	5.3
	4	78 160 162 183	1.210^*	>1000.0	NA	0.000^*	>1000.0

by introducing proximal point methodologies such as from [dO16] into the single-tree ECP framework and by employing concepts from spectral bundle methods [HR00].

5.4 Comparison between 1T-ECP-R and miSOC

Next, we compare the 1T-ECP-R tests and the miSOC tests. Qualitatively, the underlying defender subproblems associated with each of these tests are diffferent relaxations for the SDP-relaxed defender subproblem, and consequently, $\Phi_D^{SDP} \geq \Phi_{D,\mathcal{H}}^{SDP}$ and $\Phi_D^{SPD} \geq \Phi_D^{SOC}$, but no such bounding relationship is known to exist between $\Phi_{D,\mathcal{H}}^{SDP}$ and Φ_D^{SOC}.

To aid in the discussion that follows, we denote $x^{\langle \text{Method} \rangle, \langle \text{Case} \rangle, \langle \text{K} \rangle}$ to be the solution generated in the test using a given method applied to a given case instance with budget K. Furthermore, we note that when 1T-ECP-R terminates with optimality, the optimal values computed have value $\Phi_{\mathcal{H}}^{SDP}$ due to Proposition 5 and Theorem 1. For comparison with the miSOC experiments, however, we report in the 1T-ECP-R section of Table 5 the incumbent value of ϕ^{SOC}.

We draw the following conclusions from Tables 4 and 5 and Figure 1 regarding the 1T-ECP-R and miSOC tests. First, the entries of Table 4 and the plots of Figure 1 suggest that 1T-ECP-R is consistently faster in reaching optimal convergence than is miSOC for the test instances with budget $K > 2$. However, this speedup comes with the following tradeoff. We see from Table 5 and Figure 1 the tendency (though not theoretically established) for $\phi_{\mathcal{H}}^{SDP}$ to underestimate ϕ^{SDP} more severely than ϕ^{SOC}. For the IEEE Case 57

Table 4: Computational performance of 1T-ECP-R and miSOC for all the test instances (IEEE Case 30, 57, 118, 300; Pegase 1354, 2869

Case		1T-ECP-R					miSOC		
	K	Cuts	% Time	Nodes	Secs/N	Secs	Nodes	Secs/N	Secs
30	1	4	33.3	23	0.13	3	52	0.02	1
	2	4	33.3	1	3.00	3	92	0.01	1
	3	4	33.3	35	0.09	3	574	0.01	8
	4	4	47.4	7	0.43	3	1012	0.01	15
57	1	4	33.3	65	0.05	3	88	0.02	2
	2	4	33.3	143	0.02	3	982	0.03	25
	3	180	40.0	357	0.01	5	5324	0.03	140
	4	313	68.8	695	0.02	16	9350	0.03	282
118	1	224	28.6	34	0.21	7	26	0.12	3
	2	234	11.1	1071	0.02	18	128	0.09	12
	3	235	20.0	288	0.03	10	278	0.10	29
	4	246	4.5	3698	0.01	44	1526	0.10	149
300	1	217	36.0	37	0.68	25	44	0.36	16
	2	599	13.7	1568	0.09	139	778	0.29	226
	3	485	3.4	8122	0.06	500	8276	0.33	2766
	4	576	2.5	10056	0.09	917	12809	0.36	4628
1354	1	406	18.8	530	0.28	151	NA	NA	NA
	2	352	4.3	3770	0.20	738	NA	NA	NA
	3	405	8.9	2287	0.15	334	NA	NA	NA
	4	43000	2.1	2385	36.23	86400	NA	NA	NA
2869	1	1069	8.5	732	4.66	3410	NA	NA	NA
	2	1129	0.4	63218	1.22	77300	NA	NA	NA
	3	1213	0.39	57900	1.49	86400	NA	NA	NA
	4	1143	0.36	97840	0.88	86400	NA	NA	NA

instances, whereas some attacks are evaluated consistently,

$$\begin{aligned}
0.057 &= \phi^{SOC}(x^{\text{1T-ECP-R},57,1}) = \phi^{SDP}_{\mathcal{H}}(x^{\text{1T-ECP-R},57,1}) \\
0.548 &= \phi^{SOC}(x^{\text{1T-ECP-R},57,2}) = \phi^{SDP}_{\mathcal{H}}(x^{\text{1T-ECP-R},57,2}) \\
0.820 &= \phi^{SOC}(x^{\text{1T-ECP-R},57,3}) = \phi^{SDP}_{\mathcal{H}}(x^{\text{1T-ECP-R},57,3}) \\
1.235 &= \phi^{SOC}(x^{\text{1T-ECP-R},57,4}) = \phi^{SDP}_{\mathcal{H}}(x^{\text{1T-ECP-R},57,4}),
\end{aligned}$$

we have other attacks

$$\begin{aligned}
0.343 &= \phi^{SOC}(x^{\text{miSOC},57,1}) > \phi^{SDP}_{\mathcal{H}}(x^{\text{miSOC},57,1}) = 0 \\
0.759 &= \phi^{SOC}(x^{\text{miSOC},57,2}) > \phi^{SDP}_{\mathcal{H}}(x^{\text{miSOC},57,2}) = 0 \\
1.017 &= \phi^{SOC}(x^{\text{miSOC},57,3}) > \phi^{SDP}_{\mathcal{H}}(x^{\text{miSOC},57,3}) = 0 \\
1.579 &= \phi^{SOC}(x^{\text{miSOC},57,4}) > \phi^{SDP}_{\mathcal{H}}(x^{\text{miSOC},57,4}) = 0
\end{aligned}$$

that illustrate the tendency of $\phi^{SDP}_{\mathcal{H}}$ to underestimate the values of attacks for this test instance that were otherwise identified as having optimal value with respect to ϕ^{SOC}. A similar effect can be observed for the IEEE Case 300, $K = 3, 4$ instances, where the attacks computed in the miSOC test $x^{\text{miSOC},300,3}$ and $x^{\text{miSOC},300,4}$ are different from corresponding attacks $x^{\text{1T-ECP-R},300,3}$ and $x^{\text{1T-ECP-R},300,4}$ computed in the 1T-ECP-R tests. These observations motivate the need to tighten the relaxation of formulation (33) that is used in deriving the single-level reformulation (34). Nevertheless, for all other instances where both 1T-ECP-R and miSOC produce solutions, the solutions and their values are the same. Furthermore, for the two Pegase instances under consideration for all budgets, the application of Mosek to (31) terminates early because of running out of memory, and no solution is generated. This is indicated in Tables 4 and 5 as NA for the corresponding miSOC test entries. In contrast, 1T-ECP-R tests are able to produce solutions with substantial attack value for the larger 1354 and 2869 Pegase instances.

The use of the relaxed defender subproblem function $\phi^{AC}_{\mathcal{H}}$ reduces the dimension of the solution space for problem (24) by $2|L|$ and allows for the elimination of some of the McCormick inequality constraints; this is

Table 5: IEEE Case 30, 57, 118, 300; Pegase 1354, 2869 tests. Values of ϕ^{SOC} with $*$ superscript indicate possibly suboptimal values due to the test reaching the allotted time limit.

Case		1T-ECP-R			miSOC		
	K	Lines Cut	ϕ_{SOC}	% Gap	Lines Cut	ϕ^{SOC}	% Gap
30	1	34	0.058	0.0	34	0.058	0.0
	2	10 40	0.600	0.0	10 40	0.600	0.0
	3	10 34 40	0.658	0.0	10 34 40	0.658	0.0
	4	8 9 10 40	0.937	0.0	8 9 10 40	0.937	0.0
57	1	45	0.057	0.0	41	0.343	0.0
	2	63 65	0.548	0.0	41 80	0.759	0.0
	3	38 41 80	0.820	0.0	33 41 80	1.017	0.0
	4	33 41 48 80	1.235	0.0	60 65 66 72	1.579	0.0
118	1	183	0.84	0.0	183	0.840	0.0
	2	121 125	1.448	0.0	121 125	1.447	0.0
	3	121 125 183	2.288	0.0	121 125 183	2.288	0.0
	4	121 125 183 184	2.568	0.0	121 125 183 184	2.567	0.0
300	1	208	8.047	0.0	208	8.047	0.0
	2	208 316	12.567	0.0	208 316	12.568	0.0
	3	208 258 263	17.239	0.0	208 224 404	17.412	0.0
	4	268 305 308 309	22.408	0.0	177 181 182 208	23.294	0.0
1354	1	601	6.667	0.0	NA	0.000	NA
	2	206 207	21.746	0.0	NA	0.000	NA
	3	206 207 452	28.413	0.0	NA	0.000	NA
	4	206 207 455 922	35.079^*	35.2	NA	0.000	NA
2869	1	4525	11.541	0.0	NA	0.000	NA
	2	4522 4525	19.706	0.0	NA	0.000	NA
	3	2176 4522 4525	26.372^*	667.5	NA	0.000	NA
	4	1475 1706 4522 4525	33.039^*	255.6	NA	0.000	NA

the cause both for the improved tractability and for the potential underestimation in evaluating each attack as compared with the miSOC solution approach.

Note that the relaxation employed in the 1T-ECP-R tests as developed in Section 3.3 may be applied to the miSDP or miSOC approaches also. Preliminary tests, which are not reported here, suggest that these relaxations have little to no significant benefit in terms of running time for the miSDP and miSOC approaches. The reason is likely attributable to the relative lack of maturity in presolving technology for SOC and SDP solvers, whereas for the linear mixed-integer instances of the master problem in the 1T-ECP-AC approach, the presolver can effectively allow for a reduction in the dimension of the solution space.

6 Conclusions

We make contributions toward the problem of identifying substantial contingencies of an AC power flow network. The problem is modeled as a maximin problem, where the lower-level problem seeks to optimally respond to a parameterized attack, which is a decision variable in the upper-level attacker's maximization problem. The method is based on a single-tree variant of the generalized extended cutting plane method [EMW14] applied to a single-level Lagrangian dual reformulation of the maximin problem. The ECP analysis accommodates the presence of integer-restricted variables and constraints that cannot be defined with a finite number of smooth functions. Our application of ECP requires solving only mixed-integer linear subproblems and minimum eigenvalue/eigenvector problems. We demonstrate the implementation and application of ECP to the dual single level reformulation.

We show that the Lagrangian dual reformulation of the defender subproblem has a zero duality gap (under mild constraint qualifications) to the corresponding maximin problem with SDP relaxation applied to the lower-level AC power flow problem. The resulting dual problem is an SDP problem that is substantially more difficult than its second-order cone relaxation analog developed in [WCA18].

The generalized ECP approach encounters the same drawbacks of any cutting plane method, such as

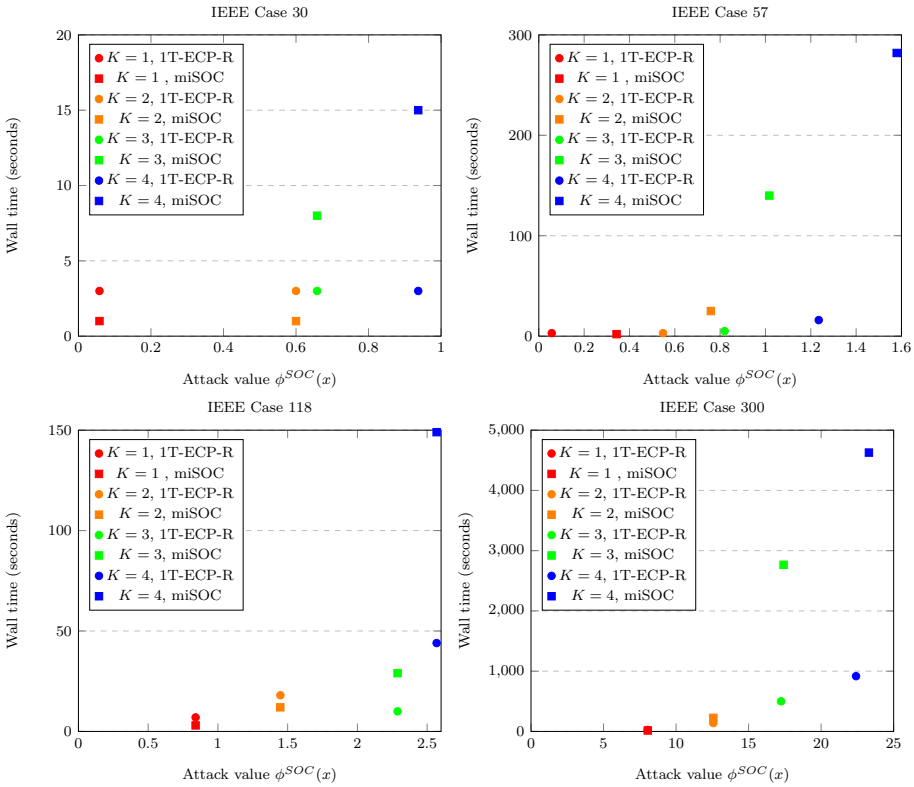

Figure 1: Comparing attack values against runtime for 1T-ECP-R and miSOC tests.

requiring an exponential number of cuts to adequately model the nonlinear, nonsmooth function that requires approximation. Nevertheless, this approach has potential for improvement, which may be found in utilizing proximal point bundle methodologies, cut aggregation, and improvement in branching rules.

The generalized ECP approach pairs particularly well with a new type of relaxation to the defender subproblem, which relaxes the restriction that complex voltage settings place on the determination of complex line flow. This relaxation is applied to the active lines only or a subset thereof. Such a relaxation is fundamentally different from relaxations such as SDP and SOC that are based on the structure of the allowable product values of bus voltages. Combining the generalized ECP approach with the line power flow relaxations yields an approach that is fundamentally different from, yet competitive with, the SOC approach developed in [WCA18], and also scales to larger problem instances.

Future work is as follows. First, better management of the generation of cutting planes is needed, since the increasing number of cuts, most of them dense, is a substantial reason for the observed increase in the master problem solution update time. In particular, cut aggregation can help. Second, the incorporation of proximal point methodologies such as spectral bundle methods, although they introduce nonlinearity, is worth analyzing within the ECP framework. Third, refinement in the process by which the master problem branch-and-cut tree develops can be motivated by the observation that the mixed-integer SDP tests require few nodes and usually produce better quality solutions within the allowed time frame. Analyzing approaches that interpolate the features of the generalized ECP approach and the mixed-integer SDP approach may help. More development and understanding of the relaxations based on the structure of the line power flows also may allow for tightened relaxations, while keeping the improved tractability obtained for the application of generalized ECP.

Acknowledgments

This material is based upon work supported by the U.S. Department of Energy, Office of Science and Office of Electricity Delivery & Energy Reliability, Advanced Grid Research and Development, under contract number DE-AC02-06CH11357. We gratefully acknowledge the computing resources provided on Bebop, a

high-performance computing cluster operated by the Laboratory Computing Resource Center at Argonne National Laboratory.

References

[Arr10] José Manuel Arroyo. Bilevel programming applied to power system vulnerability analysis under multiple contingencies. *IET Generation, Transmission & Distribution*, 4(2):178–190, 2010.

[BV10] Daniel Bienstock and Abhinav Verma. The $n - k$ problem in power grids: New models, formulations, and numerical experiments. *SIAM Journal on Optimization*, 20(5):2352–2380, 2010.

[BWFW08] X. Bai, H. Wei, K. Fujisawa, and Y. Wang. Semidefinite programming for optimal power flow problems. *International Journal of Electrical Power & Energy Systems*, 30(6):383–392, 2008.

[CHH16] C. Coffrin, H. L. Hijazi, and P. Van Hentenryck. The QC relaxation: A theoretical and computational study on optimal power flow. *IEEE Transactions on Power Systems*, 31(4):3008–3018, 2016.

[Cla90] F. Clarke. *Optimization and Nonsmooth Analysis*. Society for Industrial and Applied Mathematics, 1990.

[DHL17] Iain Dunning, Joey Huchette, and Miles Lubin. JuMP: A modeling language for mathematical optimization. *SIAM Review*, 59(2):295–320, 2017.

[DKPVK15] S. Dempe, V. Kalashnikov, G.A. Pérez-Valdés, and N. Kalashnykova. *Bilevel Programming Problems: Theory, Algorithms and Applications to Energy Networks*. Springer Publishing Company, Incorporated, 2015.

[dO16] Welington de Oliveira. Regularized optimization methods for convex MINLP problems. *TOP*, 24(3):665–692, 2016.

[EMW14] Ville-Pekka Eronen, Marko M. Mäkelä, and Tapio Westerlund. On the generalization of ECP and OA methods to nonsmooth convex MINLP problems. *Optimization*, 63(7):1057–1073, 2014.

[GLRT99] Nicholas IM Gould, Stefano Lucidi, Massimo Roma, and Philippe L Toint. Solving the trust-region subproblem using the Lanczos method. *SIAM Journal on Optimization*, 9(2):504–525, 1999.

[GPU18] T. Gally, M.E. Pfetsch, and S. Ulbrich. A framework for solving mixed-integer semidefinite programs. *Optimization Methods and Software*, 33(3):594–632, 2018.

[Hag01] W. Hager. Minimizing a quadratic over a sphere. *SIAM Journal on Optimization*, 12(1):188–208, 2001.

[Hel02] C. Helmberg. Semidefinite programming. *European Journal of Operational Research*, 137(3):461 – 482, 2002.

[HR00] C. Helmberg and F. Rendl. A spectral bundle method for semidefinite programming. *SIAM Journal on Optimization*, 10(3):673–696, 2000.

[IBM] IBM Corporation. *IBM ILOG CPLEX V12.7*. Accessed 1 Nov. 2018.

[Jab06] R. A. Jabr. Radial distribution load flow using conic programming. *IEEE Transactions on Power Systems*, 21(3):1458–1459, 2006.

[Kim17] Kibaek Kim. An optimization approach for identifying and prioritizing critical components in a power system. Technical Report ANL/MCS-P7076-0717, Argonne National Laboratory, 2017.

[LL12] J. Lavaei and S. H. Low. Zero duality gap in optimal power flow problem. *IEEE Transactions on Power Systems*, 27(1):92–107, 2012.

[McC76] G.P. McCormick. Computability of global solutions to factorable nonconvex programs: Part I — Convex underestimating problems. *Mathematical Programming*, 10(1):147–175, 1976.

[MHLD13] Daniel K Molzahn, Jesse T Holzer, Bernard C Lesieutre, and Christopher L DeMarco. Implementation of a large-scale optimal power flow solver based on semidefinite programming. *IEEE Transactions on Power Systems*, 28(4):3987–3998, 2013.

[MOS19] MOSEK ApS. *MOSEK Optimizer API for C 9.0.97*, 2019.

[NER04] NERC Steering Group. Technical Analysis of the August 14, 2003, Blackout: What Happened, Why, and What Did We Learn? Technical report, North American Electric Reliability Council, 2004.

[oWDoEE99] University of Washington-Department of Electrical Engineering. Power systems test case archive, 1999. Accessed 7 Nov. 2018.

[Pha12] Dzung T Phan. Lagrangian duality and branch-and-bound algorithms for optimal power flow. *Operations Research*, 60(2):275–285, 2012.

[PMDL10] A. Pinar, J. Meza, V. Donde, and B. Lesieutre. Optimization strategies for the vulnerability analysis of the electric power grid. *SIAM Journal on Optimization*, 20(4):1786–1810, 2010.

[QG92] I. Quesada and I.E. Grossmann. An LP/NLP based branch and bound algorithm for convex MINLP optimization problems. *Computers & Chemical Engineering*, 16(10):937–947, 1992. An International Journal of Computer Applications in Chemical Engineering.

[SWB09] Javier Salmeron, Kevin Wood, and Ross Baldick. Worst-case interdiction analysis of large-scale electric power grids. *IEEE Transactions on Power Systems*, 24(1):96–104, 2009.

[Tan11] O. Tange. GNU parallel - the command-line power tool. *;login: The USENIX Magazine*, 36(1):42–47, Feb 2011.

[U.S04] U.S./Canada Power System Outage Task Force. Final Report on the August 14, 2003 Blackout in the United States and Canada: Causes and Recommendations. Technical report, Office of Electricity Delivery & Energy Reliability—United States Department of Energy, 2004.

[WCA18] X. Wu, A.J. Conejo, and N. Amjady. Robust security constrained ACOPF via conic programming: Identifying the worst contingencies. *IEEE Transactions on Power Systems*, 33:5884–5891, 2018.

[WP95a] T. Westerlund and F. Pettersson. An extended cutting plane method for solving convex MINLP problems. *Computers & Chemical Engineering*, 19:131–136, 1995.

[WP95b] Tapio Westerlund and Frank Pettersson. An extended cutting plane method for solving convex MINLP problems. *Computers & Chemical Engineering*, 19:131–136, 1995.

[ZFP+17] Yang Zheng, Giovanni Fantuzzi, Antonis Papachristodoulou, Paul Goulart, and Andrew Wynn. Fast ADMM for semidefinite programs with chordal sparsity. In *2017 American Control Conference (ACC)*, pages 3335–3340. IEEE, 2017.

[ZMS18] R.D. Zimmermann and C.E. Murillo-Sánchez. *Matpower 7.0b1 User's Manual*. Power Systems Engineering Research Center (PSerc), 2018.

[ZZ13] Long Zhao and Bo Zeng. Vulnerability analysis of power grids with line switching. *IEEE Transactions on Power Systems*, 28(3):2727–2736, 2013.